Advances in Chemical Engineering and Science, 2016, 6, 364-378
http://www.scirp.org/journal/aces
ISSN Online: 2160-0406
ISSN Print: 2160-0392

Morphological and Electrochemical Characterization of $Ti/M_xTi_ySn_zO_2$ (M = Ir or Ru) Electrodes Prepared by the Polymeric Precursor Method

Jussara F. Carneiro[1], Jéssica R. Silva[2], Robson S. Rocha[3], Josimar Ribeiro[2*], Marcos R. V. Lanza[1]

[1]Instituto de Química de São Carlos, USP-Universidade de São Paulo, São Carlos, SP, Brazil
[2]Departamento de Química, UFES-Universidade Federal do Espírito Santo, Vitória, ES, Brazil
[3]Escola de Engenharia de São Carlos, USP-Universidade de São Paulo, São Carlos, SP, Brazil
Email: *josimar.ribeiro@ufes.br

How to cite this paper: Carneiro, J.F., Silva, J.R., Rocha, R.S., Ribeiro, J. and Lanza, M.R.V. (2016) Morphological and Electrochemical Characterization of $Ti/M_xTi_ySn_zO_2$ (M = Ir or Ru) Electrodes Prepared by the Polymeric Precursor Method. *Advances in Chemica Engineering and Science*, **6**, 364-378.
http://dx.doi.org/10.4236/aces.2016.64037

Received: June 28, 2016
Accepted: September 27, 2016
Published: September 30, 2016

Abstract

This paper describes the effect of the composition of the oxide films on the properties of electrodes $Ti/M_xTi_ySn_zO_2$ (M = Ir or Ru) prepared by the polymeric precursor method. XRD studies showed that the anodes are formed by solid solutions. The electrodes containing IrO_2 exhibit lower activity for the oxygen evolution reaction. The doping of the electrode surface with SnO_2 improves the catalytic properties of the anodes. However, it should be held in appropriate compositions, because the change in the atomic ratio of this element shows a marked effect on the stability of the oxides. Electrode $Ti/Ir_{0.2}Ti_{0.3}Sn_{0.5}O_2$ has lower lifetime, *i.e.* 6 hours. The 20% decrease in the stoichiometric amount of SnO_2 increases the time to a value above 70 hours, as observed for $Ti/Ir_{0.3}Ti_{0.4}Sn_{0.3}O_2$. Electrode $Ti/Ru_{0.3}Ti_{0.4}Sn_{0.3}O_2$ shows lifetime of 11 hours; therefore IrO_2 is more stable than RuO_2 under the conditions investigated. These results suggest that electrode $Ti/Ir_{0.3}Ti_{0.4}Sn_{0.3}O_2$ is promising for different applications, such as water electrolysis, capacitors and organic electrosynthesis.

Keywords

Dimensionally Stable Anodes (DSA), Oxide Films, Electrochemical Properties, Polymeric Precursor Method

1. Introduction

Oxide electrodes have been technologically important since the discovery of dimensionally stable anodes (DSA®) by Beer [1] and their applications in chlor-alkali industries. These electrodes constitute a mixture of oxides frequently prepared by standard thermal decomposition (SD) of metallic precursor salts in aqueous or alcohol solution, supported by metallic titanium [2].

The electro-catalytic properties of metal oxides are associated with electronic and geometric factors [3]. The electronic factor is related to the chemical composition of the film, hence the physico-chemical properties of the constituent oxides, affecting the adhesion strength surface/intermediate. The geometric factor is directly related to the morphology of the film.

Research has been conducted to find new materials and procedures to improve the performance of DSA, for example, thermal decompositon of iridium and/or ruthenium precursor salts [4] [5], thermal decomposition of hydroxo-aceto-chloro-based precursors [6], Ti/TiO_2 nanotubes prepared by anodization method [7] spin coating deposition technique [8]. The total or partial deactivation of thin films prepared by SD can be observed when they operate under drastic conditions and in a short period of time [4] [9] [10]. Electrodes as Ti/RuO_2 and Ti/IrO_2, prepared by the decomposition of polymeric precursors (Pechini method) [11], have shown better electrochemical activity, *i.e.* longer life and higher active area than those prepared by the method of chlorides [12]-[14]. Moreover, the chemical or mechanical stability of oxide electrodes can be enhanced by incorporating/doping other metal ions into the films [3].

The polymeric precursor method consists in the formation of chelates between metal cations and carboxylic acid and subsequent polymerization by a polyesterification reaction with polyalcohol [15]. The central idea is to distribute the cations throughout the polymeric structure. Heat treatment causes the release of organic matter and the formation of crystallites duly ordained [16]. This result is particularly interesting when the aims are to obtain materials with high crystallinity and controlled distribution of the constituents in the crystalline lattice.

This study investigates the morphological and electrochemical properties of oxide electrodes Ti/$Ir_{0.3}Ti_{0.4}Sn_{0.3}O_2$; Ti/$Ir_{0.2}Ti_{0.3}Sn_{0.5}O_2$ and Ti/$Ru_{0.3}Ti_{0.4}Sn_{0.3}O_2$ prepared by the thermal decomposition of polymeric precursors.

2. Experimental

2.1. Preparation of Electrodes

Thin film electrodes of nominal compositions $Ir_{0.3}Ti_{0.4}Sn_{0.3}O_2$, $Ir_{0.2}Ti_{0.3}Sn_{0.5}O_2$ and $Ru_{0.3}Ti_{0.4}Sn_{0.3}O_2$ were prepared by the thermal decomposition of a polymeric precursor solution (DPP) [11]. This method consists in synthesizing resins of metallic precursors by mixing citric acid (CA) in ethylene glycol (EG). The Ru, Ir, Sn, and Ti resins were prepared separately. First, 8 g of citric acid (Merk) were dissolved in 9 mL ethylene glycol (Merk) at 60˚C - 65˚C. After the dissolution of the acid, a solution of the precursor metal in isopropanol with 0.1 mol·L^{-1} concentration ($RuCl_3 \cdot xH_2O$, $IrCl_3 \cdot xH_2O$, $TiCl_2 \cdot 6H_2O$ all purchased from Aldrich and $C_6H_5O_7Sn_2$ synthesized from $SnCl_2$ (Aldrich), as described in [17]), was added to the CA/EG solution. The temperature was then raised up to 85˚C - 90˚C and the solution under was kept under rigorous stirring (300 rpm) for 1 - 2 hours for esterification and total isopropanol evaporation.

The precursor solutions were deposited on both sides of the pretreated metallic titanium (2.5 × 2.5 cm) by brushing, as described in the literature [12]. After the application of the coating, the electrodes were dried at 130˚C for 5 minutes and then calcined at 450˚C for 5 minutes. This procedure was repeated until the desired mass (125 mg·cm^{-2}) had been achieved. The layers were finally annealed at 450˚C for 1 hour under air flow.

2.2. Morphological and Electrochemical Characterizations

This measurement and others are deliberate, using specifications that anticipate your paper as one part of the entire journals, and not as an independent document. Please do not revise any of the current designations. The crystalline structures were physically characterized by X-ray diffraction (XRD) using an XRD-6000 diffractometer (Shimadzu) with a CuKα radiation source (λ = 1.5406 Å) operating in the continuous scan mode (4˚ min^{-1}) from 10˚ to 90˚.

The surface morphology and microstructure of the deposited oxide films were analyzed through optical microscopy and scanning electron microscopy (SEM). Photomicrographs were obtained by a Zeiss LEO model 440 SEM coupled to an OXFORD operating with electron beam of 15 kV. The average composition was analyzed by PGT PRISM energy dispersive X-ray spectrometer (EDX) coupled to the SEM instrument.

2.3. Electrochemical Measurements

Electrochemical experiments were conducted with AUTOLAB model PGSTAT30 instrumentation. Voltammetric curves were recorded at scan rate of 50 mV·s^{-1} using 0.5 mol·dm^{-3} of H_2SO_4 as the supporting electrolyte. A platinum foil served as the auxiliary electrode and the KCl saturated calomel electrode (SCE) was used as the reference. The cell was thermostated at 25˚C.

Impedance spectra were recorded at constant potential between 0.3 and 1.4 V vs Ag/AgCl. Electrochemical impedance spectroscopy (EIS) measurements were obtained in the 5 mHz - 10 kHz frequency interval using the "single sine" method and a sine wave amplitude of 5 mV (p/p). An AUTOLAB software program (FRA analyzer) was used for the analysis of the impedance data.

The stability of the electrodes was assessed based on their lifetime (LT) under galvanostatic conditions at a high current density (400 mA·cm^{-2}) in 0.5 mol·dm^{-3} of H_2SO_4. The electrode lifetime was considered the time necessary for the electrode potential to achieve a value of 8.0 V.

3. Results and Discussion

3.1. Morphological and Chemical Characterizations

Figure 1 shows the XRD patterns for different compositions of electrodes prepared at 450˚C. In the electrodes containing iridium, characteristic diffraction peaks were

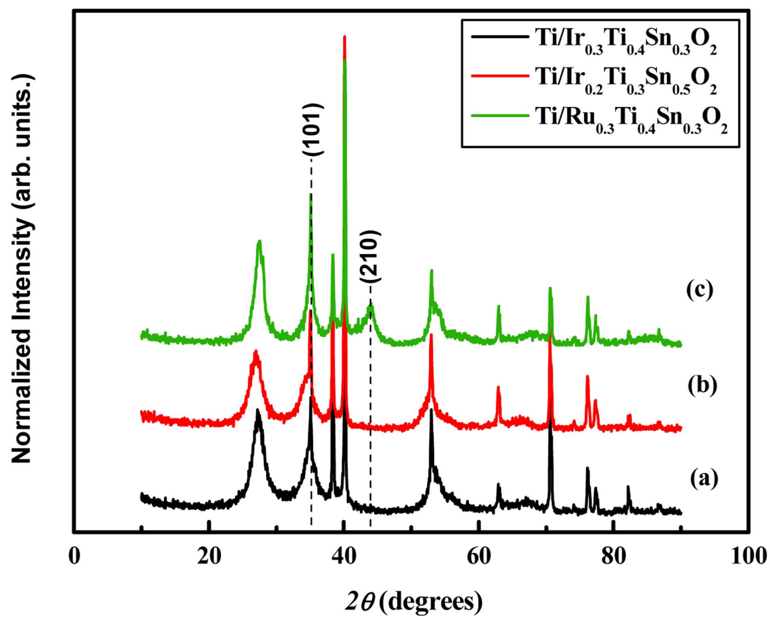

Figure 1. XRD patterns obtained for the oxide electrodes with different nominal compositions (a) $Ti/Ir_{0.3}Ti_{0.4}Sn_{0.3}O_2$; (b) $Ti/Ir_{0.2}Ti_{0.3}Sn_{0.5}O_2$; (c) $Ti/Ru_{0.3}Ti_{0.4}Sn_{0.3}O_2$.

observed and attributed to IrO_2, according to JCPDS PDF #15-0870. $Ti/Ru_{0.3}Ti_{0.4}Sn_{0.3}O_2$ showed two peaks, one at $2\theta = 43.7˚$ and another at $2\theta = 53.6˚$, which correspond to RuO_2 JCPDS PDF #40-1290. However, by comparing the positions of the peaks in the XRD obtained with the respective pure oxide, it is possible to observe that Sn-rich electrode composition displays peaks shifted toward the pure SnO_2 pattern JCPDS PDF #46-1088, indicating that Ir and/or Ti atoms may be incorporated into the SnO_2 crystalline reticule. The opposite trend is observed for Ru-electrode composition, which have their peaks shifted toward the pure RuO_2 pattern due to the incorporation of Sn and/or Ti atoms into the RuO_2 crystalline reticule. All samples displayed typical crystalline characteristics of tetragonal, with space group P42/nm. All those evidences suggesting the formation of a saturated solid solution for all the compositions investigated, one for Ir/Ti/Sn and other for Ru/Ti/Sn compositions. The XRD patterns show that all materials synthesized contained the Ti phase attributed to the Ti metallic subtract.

The average crystallite sizes of the oxide particles were estimated by the Debye-Scherrer equation [18] at crystalline planes ((210): $2\theta = 43.7˚$) for $Ti/Ru_{0.3}Ti_{0.4}Sn_{0.3}O_2$, and ((101): $2\theta = 34.5˚$) for $Ti/Ir_{0.2}Ti_{0.3}Sn_{0.5}O_2$ and $Ti/Ir_{0.3}Ti_{0.4}Sn_{0.3}O_2$. The values obtained were approximately 4 and 5 nm, respectively.

The roughness of the oxides Table 1 was estimated from the optical microscopy analyses Figure 2 performed in random areas of the film (average of five analyses). The electrode with nominal composition of $Ti/Ru_{0.3}Ti_{0.4}Sn_{0.3}O_2$ showed the lowest roughness, which suggests that the morphology of the oxide layers is highly dependent on the physicochemical properties of the oxides and the nature of the precursors.

Figure 3 shows some representative SEM images of the oxide films. Films containing

Table 1. Roughness estimated for the oxide films prepared by the polymeric precursor method.

	Roughness estimated (μm)
$Ti/Ir_{0.3}Ti_{0.4}Sn_{0.3}O_2$	13.9
$Ti/Ir_{0.2}Ti_{0.3}Sn_{0.5}O_2$	12.6
$Ti/Ru_{0.3}Ti_{0.4}Sn_{0.3}O_2$	8.3

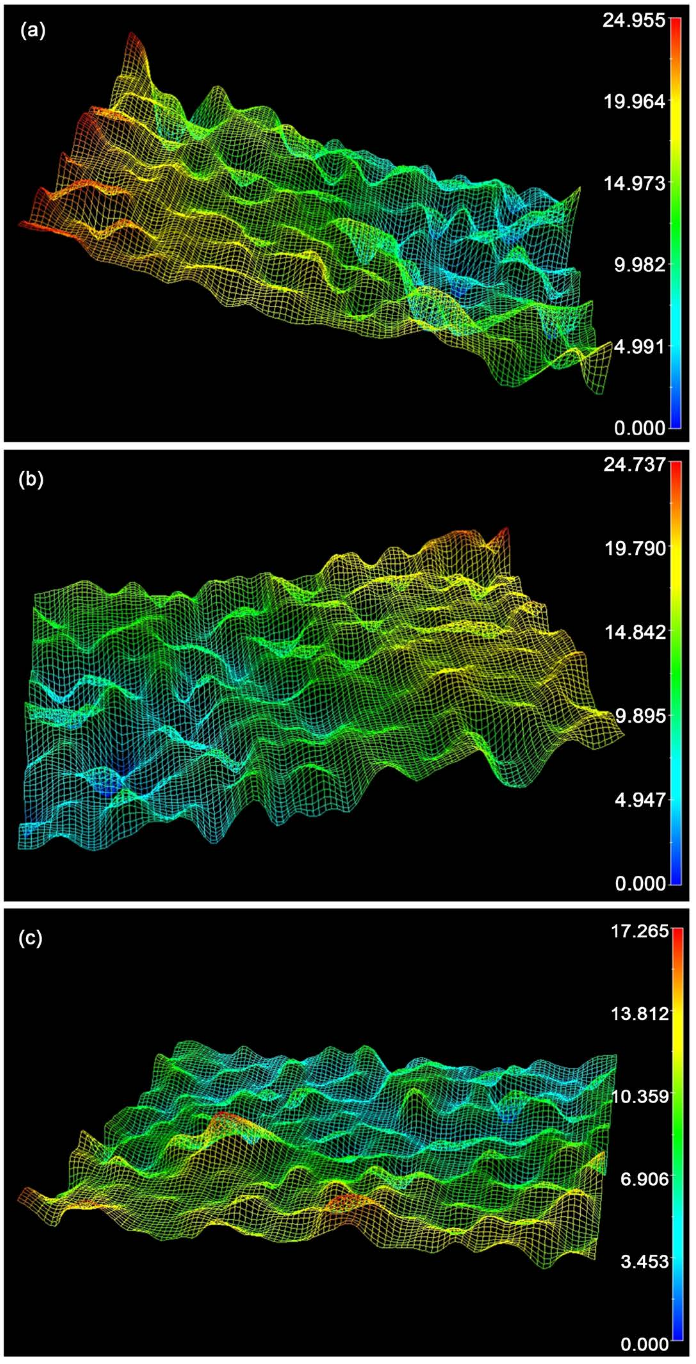

Figure 2. Optical microscopy of the oxide electrodes, original magnification 350× (a) $Ti/Ir_{0.3}Ti_{0.4}Sn_{0.3}O_2$; (b) $Ti/Ir_{0.2}Ti_{0.3}Sn_{0.5}O_2$; (c) $Ti/Ru_{0.3}Ti_{0.4}Sn_{0.3}O_2$. Beside each picture is displayed the scale in μm.

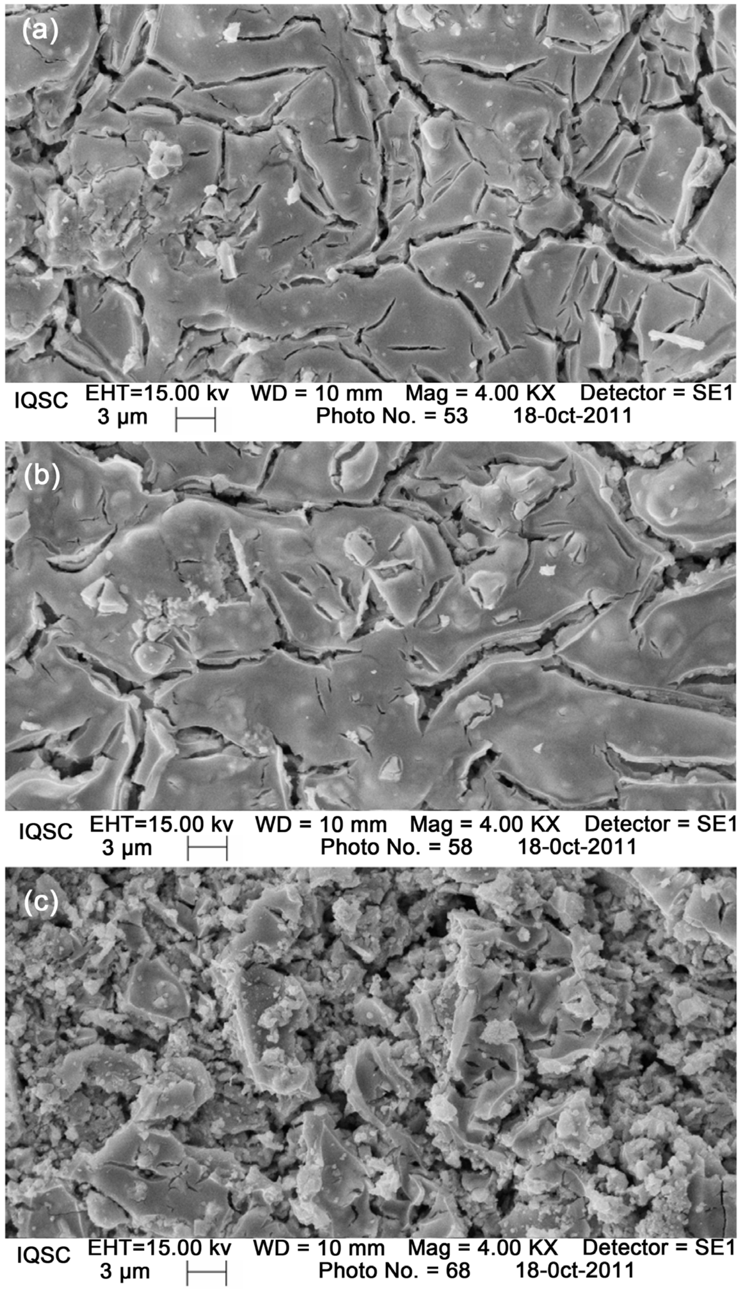

Figure 3. SEM surface image of the oxide electrodes, original magnification 4000× (a) $Ti/Ir_{0.3}Ti_{0.4}Sn_{0.3}O_2$; (b) $Ti/Ir_{0.2}Ti_{0.3}Sn_{0.5}O_2$; (c) $Ti/Ru_{0.3}Ti_{0.4}Sn_{0.3}O_2$.

IrO_2 (a, b) show uniform and continuous structures with cracks, *i.e.*, mud-cracked-type morphology which are typical of thermally prepared oxide layers [10] [12]. Moreover, one observe that due to the increase in the amount of SnO_2 in the electrode composition, cracks become larger (b), however the surface becomes less rough (see **Table 1**). However, the SEM image of the films containing RuO_2 (c) indicate a distinct morphology, and in this case, the morphology change severally where the amount of fissures and cracks increase. The oxide surface morphology shows a clear relationship with the coating compositions investigated.

Table 2 shows the EDX analyses of the micrographs Figure 3. The EDX analysis of the electrodes indicated a good correlation between experimental and nominal compositions. The control of the composition of the films can be explained by the method used, since this polymer is formed before the calcination and the metal atoms are trapped in the matrix, which hinders its evaporation and consequent loss. All electrodes exhibited a homogenous distribution of particles on the electrode surface.

3.2. Electrochemical Characterizations

Figure 4 shows the j/E curve obtained in the cyclic voltammetric experiments. This profile is typical of thermally prepared oxide layer electrodes [19] [20] and characteristic of DSA® electrodes [21]. The figure also shows a blurred peak at around 0.5 V associated with the Ru (III)/Ru(IV) redox transition [22] for the Ti/$Ru_{0.3}Ti_{0.4}Sn_{0.3}O_2$ electrode. The voltammograms of the electrodes containing IrO_2 showed a peak typical of the Ir(III)/Ir (IV) transition in the region between 0.4 and 0.8 V [6].

The oxygen evolution reaction occurs at a more positive potential for the electrode containing the largest amount of SnO_2. According to Fukunaga *et al.* [23], the doping of the electrode surface with SnO_2 is an effective strategy to improve performance even in

Table 2. Atomic ratios (%) of the oxide films with different nominal compositions.

	Ti	Ir	Ru	Sn
Ti/$Ir_{0.3}Ti_{0.4}Sn_{0.3}O_2$	50.8	25.1	-	24.1
Ti/$Ir_{0.2}Ti_{0.3}Sn_{0.5}O_2$	39.8	11.5	-	48.7
Ti/$Ru_{0.3}Ti_{0.4}Sn_{0.3}O_2$	40.6	-	36.7	22.7

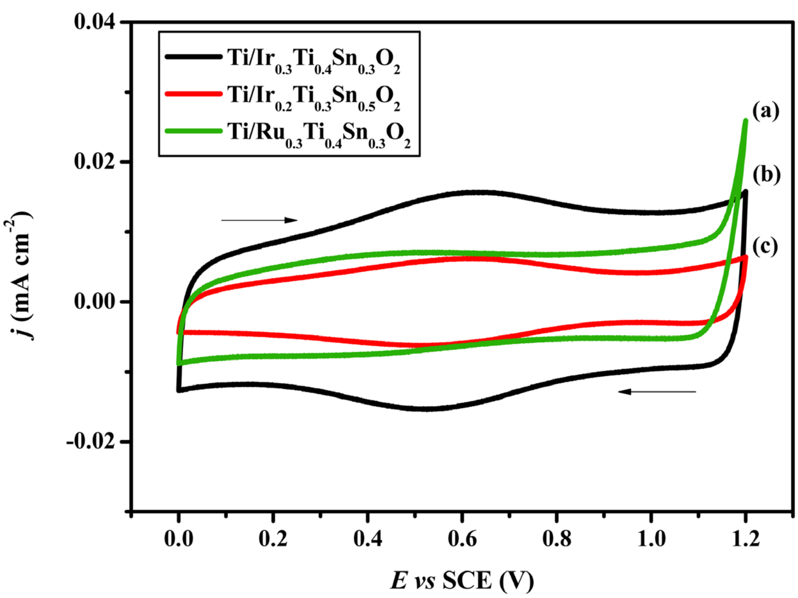

Figure 4. Cyclic voltammograms at 50 $mV \cdot s^{-1}$ in 0.5 $mol \cdot dm^{-3}$ of H_2SO_4 of the oxide electrodes *vs.* SCE (a) Ti/$Ir_{0.3}Ti_{0.4}Sn_{0.3}O_2$; (b) Ti/$Ir_{0.2}Ti_{0.3}Sn_{0.5}O_2$; (c) Ti/$Ru_{0.3}Ti_{0.4}Sn_{0.3}O_2$.

the treatment of degradation of organic compounds thus our results are in agreement with previous report.

The comparison between the electrode containing IrO_2 and those containing RuO_2 shows the IrO_2 exhibits lower activity for the oxygen evolution reaction.

The impedance behavior of the electrodes was investigated to further characterize the different Ti/$Ir_{0.3}Ti_{0.4}Sn_{0.3}O_2$; Ti/$Ir_{0.2}Ti_{0.3}Sn_{0.5}O_2$ and Ti/$Ru_{0.3}Ti_{0.4}Sn_{0.3}O_2$ systems. The Nyquist diagram (Z' *vs* Z") of the electrodes obtained between 0.3 and 1.4 V vs Ag/AgCl is shown in **Figure 5**. In the low frequency domain, electrodes Ti/$Ir_{0.3}Ti_{0.4}Sn_{0.3}O_2$ and Ti/$Ir_{0.2}Ti_{0.3}Sn_{0.5}O_2$ formed a straight line parallel to Z", characteristic of an ideally polarizable electrode, and a slight deviation from the straight line along Z", suggesting a non-ideally polarizable electrode [24] [25]. The shift from the ideal capacitor behavior is a consequence of the material's porosity [24] [26]. In the low-frequency domain region a decrease in impedance was found when the applied potentials were positively shifted. This result suggests that the EIS responses in this domain region indicate a faradaic process of the bulk redox transitions of the oxide material. The difference observed between the Ir-based electrodes and Ru-based electrodes maybe could be explained due to the higher electronic conductivity in the Ru-Ti-Sn/solution than in the Ir-Ti-Sn/solution interfaces.

The Bode plot (θ vs. log f) obtained at 0.3 V vs Ag/AgCl for electrodes is shown in **Figure 6**. An analysis of this figure indicates that the main feature of these electrodes is the appearance of a well-defined time constant (τ) for the Ti/$Ru_{0.3}Ti_{0.4}Sn_{0.3}O_2$ electrode, which is characterized by a maximum phase angle ranging from 1 to 100 Hz. This behavior can be ascribed to the large number of RuO_2 transition states contributing to the charging system [27]. This results corroborated with the Nyquist plot interpretation above because the Ru-based electrode shows more pseudo capacitive behavior than the Ir-based electrode [10] [24].

The stability of the electrodes was assessed based on their lifetime, considering the time necessary for the electrode potential to reach 8.0 V. The electrode containing larger amounts of SnO_2 (Ti/$Ir_{0.2}Ti_{0.3}Sn_{0.5}O_2$) has a shorter lifetime. The 20% decrease in the stoichiometric amount of this oxide as well as the high amount (10%) of IrO_2 (Ti/$Ir_{0.3}Ti_{0.4}Sn_{0.3}O_2$) increase the time to a value above 70 hours. Comparing the electrode Ti/$Ir_{0.3}Ti_{0.4}Sn_{0.3}O_2$ with Ti/$Ru_{0.3}Ti_{0.4}Sn_{0.3}O_2$, IrO_2 has higher stability under drastic conditions of electrolysis than RuO_2 (**Table 3**).

The lifetime of oxide electrodes is directly correlated with two factors: passivation and dissolution of the coating [21]. The first factor is due to the penetration of the electrolyte through the pores or cracks towards the substrate, resulting in the oxidation of the metallic support and forming a non-conductive layer between the substrate and the oxide coating [28]-[30]. The second factor involves the loss of electroactive material (erosion or dissolution), resulting in a gradual reduction of the voltammetric charge. This may occur due to the pores in the layer and the rapid evolution of gas on the surface, inducing the separation of weakly bound parts of the active layer [28] [31] [32].

Morphological changes of the electrode surface after the lifetime test can be observed

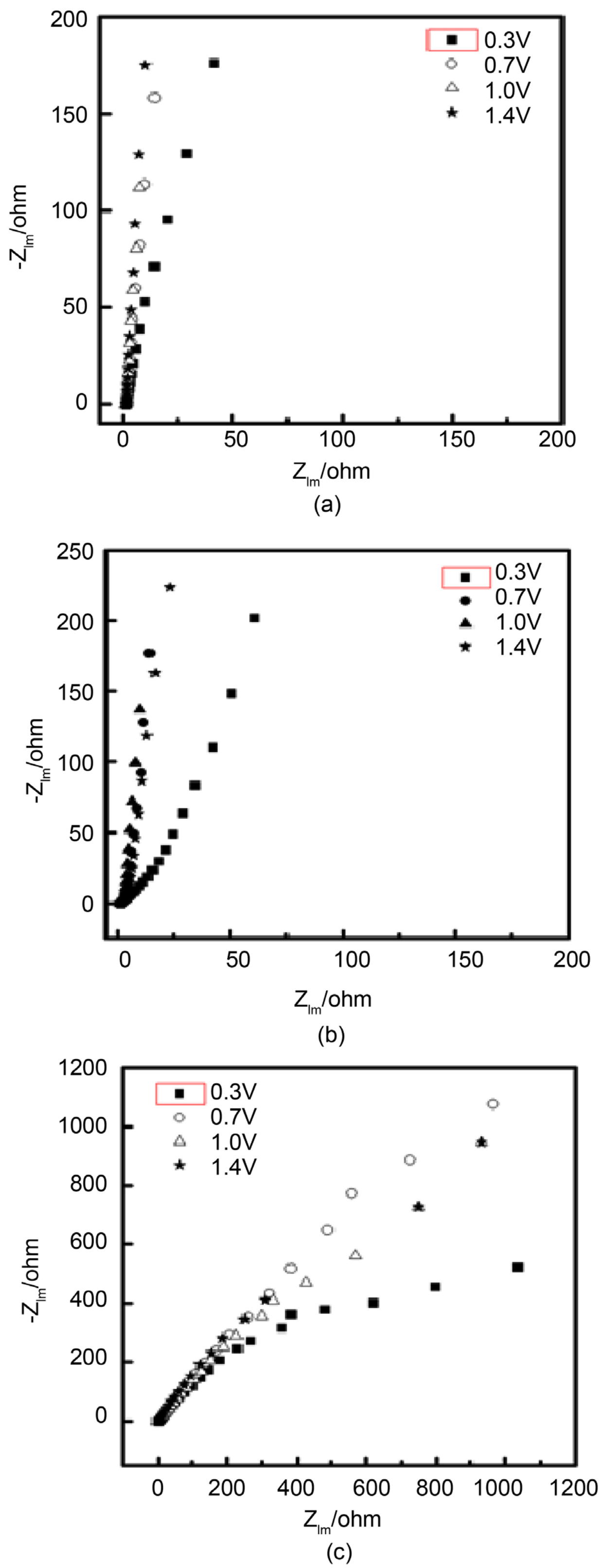

Figure 5. Nyquist diagrams of the oxide electrodes as a function of the applied potential (0.3, 0.7, 1.0 and 1.4 V) *vs.* Ag/AgCl (a) $Ti/Ir_{0.3}Ti_{0.4}Sn_{0.3}O_2$; (b) $Ti/Ir_{0.2}Ti_{0.3}Sn_{0.5}O_2$; (c) $Ti/Ru_{0.3}Ti_{0.4}Sn_{0.3}O_2$.

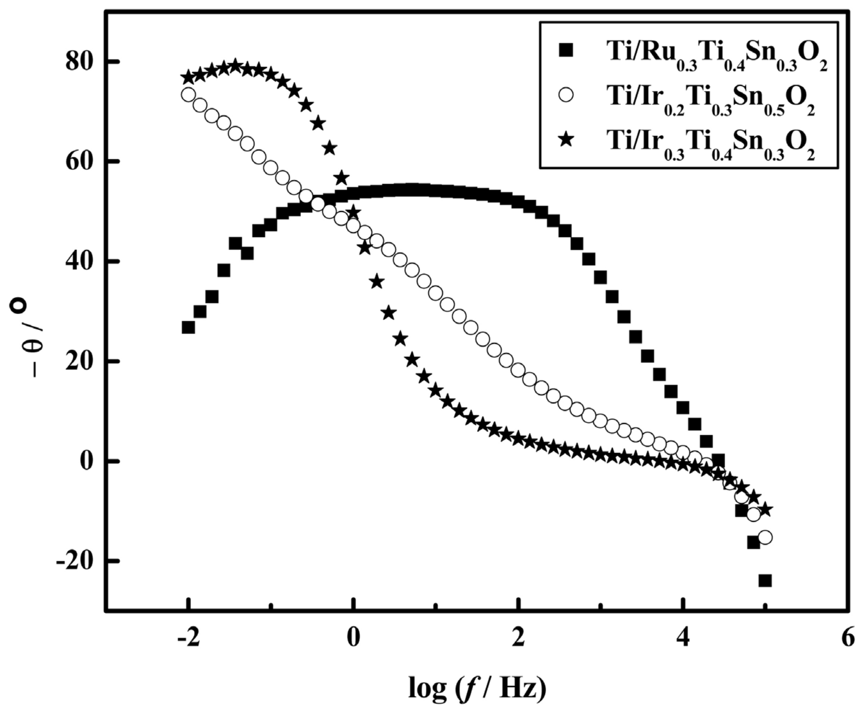

Figure 6. Bode plot at 0.3 V *vs.* Ag/AgCl as a function of the oxide electrodes. (-○-) $Ti/Ir_{0.2}Ti_{0.3}Sn_{0.5}O_2$; (-■-) $Ti/Ir_{0.3}Ti_{0.4}Sn_{0.3}O_2$ (-★-) $Ti/Ru_{0.3}Ti_{0.4}Sn_{0.3}O_2$.

Table 3. Lifetime values obtained for the oxide electrodes under galvanostatic conditions at a high current density (400 $mA \cdot cm^{-2}$) in 0.5 $mol \cdot dm^{-3}$ of H_2SO_4.

	Lifetime (h)
$Ti/Ir_{0.3}Ti_{0.4}Sn_{0.3}O_2$	>70
$Ti/Ir_{0.2}Ti_{0.3}Sn_{0.5}O_2$	6.16
$Ti/Ru_{0.3}Ti_{0.4}Sn_{0.3}O_2$	11.65

through microstructural analysis (**Figure 7**), which shows worn structures with erosion of the active layer. The EDX analysis revealed a decrease in the quantity of Ir and Ru, confirming the loss of the electroactive material, well as a decrease of Sn (**Table 4**).

The curves obtained for the lifetime showed a slow increase in the potential followed by an abrupt increase at the end of the experiment for all compositions investigated. This behavior indicates a rise in the electrode structure resistance. Such an increase may have resulted from the loss of Ir or Ru in the top layers of the electrode and/or the formation and growth of a non-conductive oxide film between the metallic substrate and the conductive oxide [9] [31].

EDX analysis after lifetime revealed a considerable increase in the titanium signal. These results suggest that besides the process of erosion, there is also a process of anodic passivation of the metallic base due to the formation of an insulating film composed primarily of TiO_x.

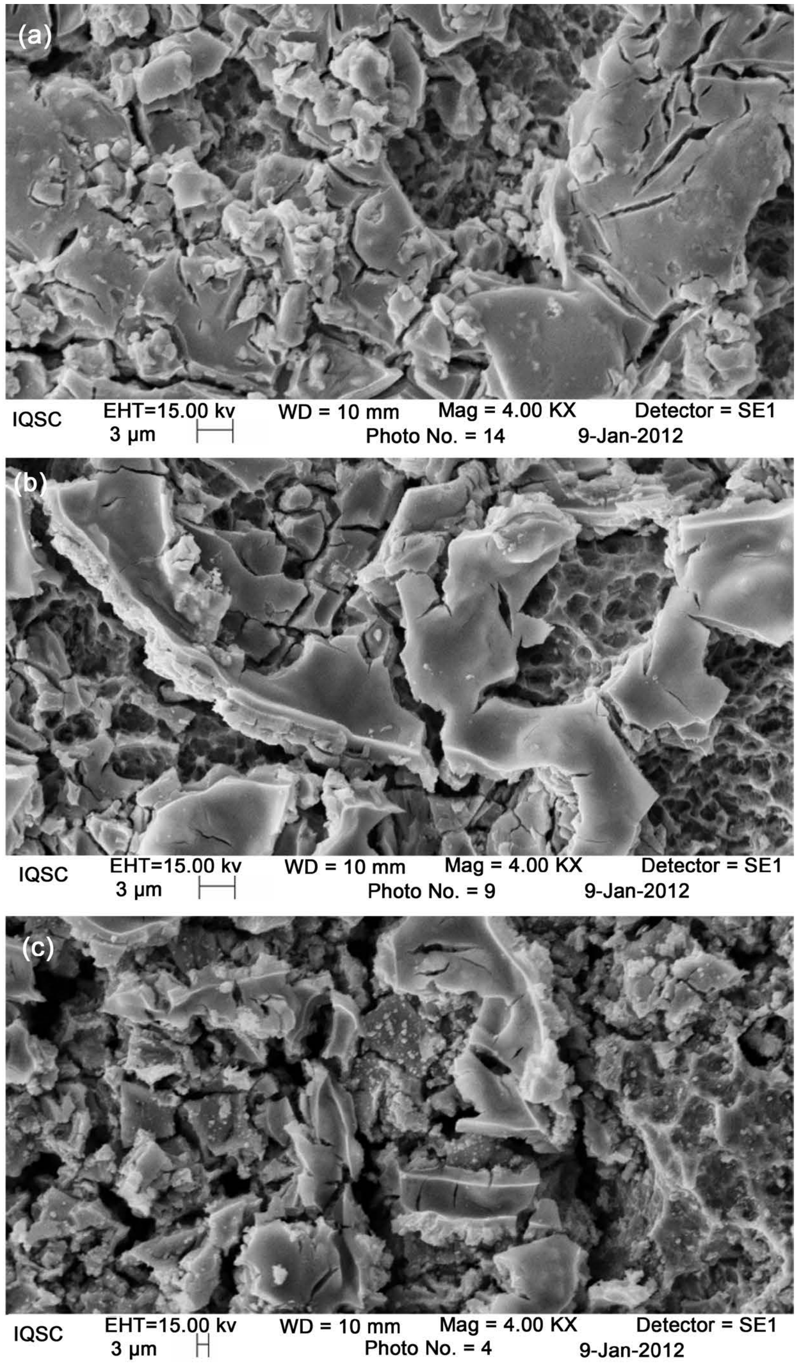

Figure 7. SEM surface image of the oxide electrodes after the lifetime test, original magnification 4000×. (a) $Ti/Ir_{0.3}Ti_{0.4}Sn_{0.3}O_2$; (b) $Ti/Ir_{0.2}Ti_{0.3}Sn_{0.5}O_2$; (c) $Ti/Ru_{0.3}Ti_{0.4}Sn_{0.3}O_2$.

Table 4. Variation in the atomic ratios (%) of the oxide films after the lifetime test.

	ΔIr (%)	ΔRu (%)	ΔSn (%)
$Ti/Ir_{0.3}Ti_{0.4}Sn_{0.3}O_2$	−10.7	-	−20.3
$Ti/Ir_{0.2}Ti_{0.3}Sn_{0.5}O_2$	−58.3	-	−61.2
$Ti/Ru_{0.3}Ti_{0.4}Sn_{0.3}O_2$	-	−72.7	−54.2

4. Conclusion

This study has demonstrated the effect of the composition of oxide films on the properties of DSA prepared by the thermal decomposition of polymeric precursors. IrO_2-based electrodes are more stable than RuO_2-based electrode under the conditions investigated and show lower activity for the oxygen evolution reaction, which makes it attractive in the oxidation of organic substances. The introduction of tin oxide in the composition film enhances the catalytic properties of the anodes. However, it should be held in appropriate compositions, because the change in the atomic ratio of this element produces marked effects on the stability of the oxides. The thin films formed are composed of a solid solution among the various oxides constituents of the film. The procedure employed for the preparation of the anodes is a good alternative to SD, minimizing the volatilization of the metal.

Acknowledgements

The authors would like to acknowledge the Conselho Nacional de Desenvolvimento Científico e Tecnológico-CNPq, the Fundação de Amparo à Pesquisa do Estado de São Paulo-Fapesp (2013/02762-5) and Fundação de Amparo à Pesquisa do Estado do Espírito Santo-FAPES for the financial support provided to this research.

References

[1] Beer, H.B. (1980) The Invention and Industrial Development of Metal Anodes. *Journal of the Electrochemical Society*, **127**, 303-307. http://jes.ecsdl.org/content/127/8/303C.abstracy http://dx.doi.org/10.1149/1.2130021

[2] Varela, H., Câmara Júnior, G.A.H.S. and Gonzalez, E.R. (2000) Oxygen Evolution Reaction on Mn_2O_3 Electrodes Supported on Stainless Steel. *Quimica Nova*, **23**, 721-726. http://www.scielo.br/scielo.php?script=sci_arttext&pid=S0100-40422000000600002 http://dx.doi.org/10.1590/S0100-40422000000600002

[3] Klink, M.J., Makgae, M.E. and Crouch, A.M. (2010) Physico-Chemical and Electrochemical Characterization of Ti/RhO_x-IrO_2 Electrodes Using Sol-Gel Technology. *Materials Chemistry and Physics*, **124**, 73-77. http://www.sciencedirect.com/science/article/pii/S0254058410003846 http://dx.doi.org/10.1016/j.matchemphys.2010.05.016

[4] Trasatti, S. (1991) Physical Electrochemistry of Ceramic Oxides. *Electrochimicam Acta*, **36,** 225-228. http://www.sciencedirect.com/science/article/pii/0013468691852442 http://dx.doi.org/10.1016/0013-4686(91)85244-2

[5] Lipkowski, J. and Ross, P.N. (1994) The Electrochemistry of Novel Materials. VCH, University of Michigan.

[6] Ferro, S., Rosestolato, D., Martínez-Huitle, C.A. and DeBattisti, A. (2014) Charge-Storage Process in IrO_2-SnO_2 Mixed-Oxide Electrodes. Role of Coating Composition, Solution pH and Temperature. *Electrochimican Acta*, **148**, 85-90. http://www.sciencedirect.com/science/article/pii/S0013468614020490 http://dx.doi.org/10.1016/j.electacta.2014.10.045

[7] Kruthika, N.L., Karthika, S., Raju, G.B. and Prabhakar, S. (2013) Efficacy of Electrocoagulation and Electrooxidation for the Purification of Wastewater Generated from Gelatin Pro-

duction Plant. *Journal of Environmental Chemical Engineering*, **1**, 183-188.
http://www.sciencedirect.com/science/article/pii/S2213343713000298
http://dx.doi.org/10.1016/j.jece.2013.04.017

[8] Fierro, C. and Comninellis, C. (2010) Kinetic Study of Formic Acid Oxidation on Ti/IrO_2 Electrodes Prepared Using the Spin Coating Deposition Technique. *Electrochimica Acta*, **55**, 7067-7071. http://www.sciencedirect.com/science/article/pii/S0013468610008820
http://dx.doi.org/10.1016/j.electacta.2010.06.066

[9] Ribeiro, J. and de Andrade, A.R. (2004) Characterization of RuO_2-Ta_2O_5 Coated Titanium Electrode Microstructure, Morphology, and Electrochemical Investigation. *Journal of the Electrochemical Society*, **151**, D106-D111. http://jes.ecsdl.org/content/151/10/D106.abstract
http://dx.doi.org/10.1149/1.1787174

[10] Tilak, B.V., Birss, V.I., Wang, J., Chen, C.P. and Rangarajan, S.K. (2001) Deactivation of Thermally Formed Ru/Ti Oxide Electrodes: An AC Impedance Characterization Study. *Journal of the Electrochemical Society*, **148**, 112-116.
http://jes.ecsdl.org/content/148/9/D112.short
http://dx.doi.org/10.1149/1.1388630

[11] Pechini, M.P. (1967) Method of Preparing Lead and Alkaline Earth Titanates and Niobates and Coating Method Using the Same to Form a Capacitor. US Patent No. 3330697.

[12] Forti, J.C., Olivi, P. and de Andrade, A.R. (2001) Characterisation of DSA®-Type Coatings with Nominal Composition Ti/$Ru_{0.3}Ti_{(0.7-x)}Sn_xO_2$ Prepared via a Polymeric Precursor. *Electrochimica Acta*, **47**, 913-917.
http://www.sciencedirect.com/science/article/pii/S0013468601007915
http://dx.doi.org/10.1016/S0013-4686(01)00791-5

[13] Terezo, A.J. and Pereira, E.C. (1999) Preparation and Characterization of Ti/RuO_2-Nb_2O_5 Electrodes Obtained by Polymeric Precursor Method. *Electrochimica Acta*, **44**, 4507-4511.
http://www.sciencedirect.com/science/article/pii/S0013468699001826
http://dx.doi.org/10.1016/S0013-4686(99)00182-6

[14] Lassali, T.A.F., Boodts, J.F.C. and Bulhoes, L.O.S. (2000) Effect of Sn-Precursor on the Morphology and Composition of $Ir_{0.3}Sn_{0.7}O_2$ Oxide Films Prepared by Sol-Gel Process. *Journal of Non-Crystalline Solids*, **273**, 129-133.
http://www.sciencedirect.com/science/article/pii/S0022309300001526
http://dx.doi.org/10.1016/S0022-3093(00)00152-6

[15] Marciel, A.P., Longo, E. and Leite, E.R. (2003) Nanostructured Tin Dioxide: Synthesis and Growth of Nanocrystals and Nanoribbons. *Quimica Nova*, **26**, 855-861.
http://quimicanova.sbq.org.br/imagebank/pdf/Vol26No6_855_13-RV02099.pdf

[16] Mourão, H.A.J.L., de Mendonça, V.R., Malagutti, A.R. and Ribeiro, C. (2009) Nanostructures in Photocatalysis: A Review about Synthesis Strategies of Photocatalysts in Nanometric Size. *Química Nova*, **32**, 2181-2186.
http://www.scielo.br/scielo.php?pid=S0100-40422009000800032&script=sci_arttext&tlng=pt
http://dx.doi.org/10.1590/S0100-40422009000800032

[17] Besso, M.M. (1965) Tin Salts of Citric Acid and Method of Preparation. US Patent No. 3213120.

[18] Klung, H.P. and Alexander, L.E. (1975) X-Ray Diffraction Procedures for Polycrystalline and Amorphous Materials. *Journal of Applied Crystallography*, **8**, 573-580.
http://scripts.iucr.org/cgi-bin/paper?S0021889875011399
http://dx.doi.org/10.1107/S0021889875011399

[19] Malpass, G.R.P., Miwa, D.W., Machado, S.A.S., Olivi, P. and Motheo, A.J. (2006) Oxidation of the Pesticide Atrazine at DSA® Electrodes. *Journal of Hazardous Materials*, **137**, 565-572.

http://www.sciencedirect.com/science/article/pii/S0304389406002160
http://dx.doi.org/10.1016/j.jhazmat.2006.02.045

[20] Motheo, A.J., Gonzalez, E.R., Tremiliosi, G., Olivi, P., de Andrade, A.R., Kokoh, B., Leger, J.M., Belgsir, E.M. and Lamy, C. (2000) The Oxidation of Formaldehyde on High Overvoltage DSA Type Electrodes. *Journal of the Brazilian Chemical Society*, **11**, 16-21. http://www.scielo.br/scielo.php?pid=S0103-50532000000100004&script=sci_arttext http://dx.doi.org/10.1590/S0103-50532000000100004

[21] Forti, J. F., Ribeiro, J., Lanza M.R.V., de Andrade, A.R. and Bertazzoli, R. (2010) Electrochemical Characterization of DSA®-Type Electrodes Using Niobium Substrate. *Electrocatalysis*, **1**, 129-138. http://link.springer.com/article/10.1007%2Fs12678-010-0020-3

[22] Ardizzone, S., Fregonara, G. and Trasatti, S. (1990) "Inner" and "Outer" Active Surface of RuO_2 Electrodes. *Electrochimica Acta*, **35**, 263-267. http://www.sciencedirect.com/science/article/pii/001346869085068X http://dx.doi.org/10.1016/0013-4686(90)85068-X

[23] Fukunaga, M.T., Guimarães, J.R. and Bertazzoli, R. (2008) Kinetics of the Oxidation of Formaldehyde in a Flow Electrochemical Reactor with TiO_2/RuO_2 Anode. *Chemical Engineering Journal*, **136**, 236-241. http://www.sciencedirect.com/science/article/pii/S1385894707002495 http://dx.doi.org/10.1016/j.cej.2007.04.006

[24] Sugimoto, W., Iwata, H., Yokoshima, K., Murakami, Y. and Takasu, Y. (2005) Proton and Electron Conductivity in Hydrous Ruthenium Oxides Evaluated by Electrochemical Impedance Spectroscopy: the Origin of Large Capacitance. *The Journal of Physical Chemistry B*, **109**, 7330-7338. http://pubs.acs.org/doi/abs/10.1021/jp044252o http://dx.doi.org/10.1021/jp044252o

[25] De Carvalho, L.A., de Andrade A.R. and Bueno, P.R. (2006) Electrochemical Impedance Spectroscopy Applied in the Study of Heterogeneous Reactions at Dimensionally Stable Anodes. *Química Nova*, **29**, 796-804. http://quimicanova.sbq.org.br/imagebank/pdf/Vol29No4_796_28-RV05188.pdf http://dx.doi.org/10.1590/S0100-40422006000400029

[26] Terezo, A.J., Bisquert, J., Pereira, E.C. and Garcia-Belmonte, G. (2001) Separation of Transport, Charge Storage and Reaction Processes of Porous Electrocatalytic IrO_2 and IrO_2/Nb_2O_5 Electrodes. *Journal of Electroanalytical Chemistry*, **508**, 59-69. http://www.sciencedirect.com/science/article/pii/S0022072801005228 http://dx.doi.org/10.1016/S0022-0728(01)00522-8

[27] Horvat-Radosevic, V., Kvastek, K., Vukovic, M. and Marijan, D. (1999) Impedance of Ruthenium Electrodes in Sulphuric Acid Solution. *Journal of Electroanalytical Chemistry*, **463**, 29-44. http://www.sciencedirect.com/science/article/pii/S0022072898004306 http://dx.doi.org/10.1016/S0022-0728(98)00430-6

[28] Martelli, G.N., Ornelas, R. and Faita, G. (1994) Deactivation Mechanisms of Oxygen Evolving Anodes at High Current Densities. *Electrochimica Acta*, **39**, 1551-1558. http://www.sciencedirect.com/science/article/pii/0013468694851344 http://dx.doi.org/10.1016/0013-4686(94)85134-4

[29] Jovanovic, V.M., Dekanski, A., Despotov, P., Nikolic, B. and Atanasoski, R.T. (1992) The Roles of the Ruthenium Concentration Profile, the Stabilizing Component and the Substrate on the Stability of Oxide Coatings. *Journal of Electroanalytical Chemistry*, **339**, 147-165. http://www.sciencedirect.com/science/article/pii/002207289280449E http://dx.doi.org/10.1016/0022-0728(92)80449-E

[30] Panic, V.V., Dekanski, A., Milonjic, S.K., Atanasoski, R.T. and Nilolic, B.Z. (1999)

RuO_2-TiO_2 Coated Titanium Anodes Obtained by the Sol-Gel Procedure and Their Electrochemical Behaviour in the Chlorine Evolution Reaction. *Colloids and Surfaces A*: *Physicochemical and Engineering Aspects*, **157**, 269-274.
http://www.sciencedirect.com/science/article/pii/S0927775799000941
http://dx.doi.org/10.1016/S0927-7757(99)00094-1

[31] Loucka, T. (1977) The Reason for the Loss of Activity of Titanium Anodes Coated with a Layer of RuO_2 and TiO_2. *Journal of Applied Electrochemistry*, **7**, 211-214.
http://link.springer.com/article/10.1007%2FBF00618987#page-1
http://dx.doi.org/10.1007/BF00618987

[32] Iwakura, C. and Sakamoto, K. (1985) Effect of Active Layer Composition on the Service Life of (SnO_2 and RuO_2) -Coated Ti Electrodes in Sulfuric Acid Solution. *Journal of the Electrochemical Society*, **132**, 2420-2423. http://jes.ecsdl.org/content/132/10/2420.short
http://dx.doi.org/10.1149/1.2113590